Decay of $^{149}Er^{g+m}$ by positron and delayed proton emission and by electron capture

R. B. Firestone, J. M. Nitschke, P. A. Wilmarth, K. Vierinen,* and J. Gilat†
Lawrence Berkeley Laboratory, University of California, Berkeley, California 94720

K. S. Toth and Y. A. Akovali
Oak Ridge National Laboratory, Oak Ridge, Tennessee 37831
(Received 6 July 1988)

In this study the decay of $^{149}Er^{g+m}$ by positron emission, electron capture, and β-delayed proton emission was investigated. Gamma rays associated with $^{149}Er^{m}$ decay were placed in a decay scheme on the basis of $\gamma\gamma$ and $x\gamma$ coincidences and half-life. We assigned 120 γ rays deexciting 91 levels in ^{149}Ho to 8.9±0.2 s $^{149}Er^{m}$ decay. The $\pi s_{1/2}$ single-particle state in ^{149}Ho was observed to occur at 49.0 keV above the $\pi h_{11/2}$ ground state. A (3.5±0.7) % isomeric transition decay branch and a (0.18±0.07) % β-delayed proton decay branch were determined for $^{149}Er^{m}$ decay. Three additional γ rays were assigned to 4±2 s $^{149}Er^{g}$ decay and a (7±2) % β-delayed proton decay branch was determined. Measured EC/β^+ ratios to proton emitting states in ^{149}Ho resulted in a $(Q_{EC}-S_p)=7.0^{+0.5}_{-0.4}$ MeV for $^{149}Er^{g}$ decay and a $S_p=1.4^{+1.0}_{-0.6}$ MeV for ^{149}Ho. The β-delayed proton spectrum from $^{149}Er^{g}$ consisted of a highly structured component corresponding to the deexcitation of levels between 4 and 5 MeV in ^{149}Ho and a structureless component corresponding to decay from higher levels. The β-strength function for $^{149}Er^{g+m}$ decay is discussed in terms of single-particle shell-model structure, weak coupling to the ^{148}Dy core, and decay of $\pi h_{11/2}$ protons across the shell closure to the $\nu h_{9/2}$ neutron orbital.

I. INTRODUCTION

The decay of $^{149}Er^{g+m}$ continues our studies of odd-mass $N=81$ nuclei which have included $^{145}Gd^{g+m}$,[1,2] $^{147}Dy^{g+m}$,[3,4] and $^{151}Yb^{g+m}$.[5] The first studies of ^{149}Er were reported by Toth *et al.*[6] and Schardt *et al.*,[7] who measured β-delayed proton activity. Schardt *et al.*[7] also constructed a partial decay scheme for $^{149}Er^{g+m}$, and Toth *et al.*[8] presented a partial isometric transition (IT) and β-decay scheme for $^{149}Er^{g+m}$. In this paper we present a more extensive decay scheme with identification of the excitation energy of the $\pi s_{1/2}$ single-particle level with respect to the $\pi h_{11/2}$ ground state. The absolute EC+β^+, IT, and the delayed proton branching intensities from $^{149}Er^{g}$ and $^{149}Er^{m}$ are reported here. We also compare the exerimental results with the predictions of a simple single-particle plus weak-coupling model.

II. EXPERIMENTAL METHODS

Both $^{149}Er^{g}$ and $^{149}Er^{m}$ were produced by the $^{58}Ni(^{94}Mo,2pn)$ reaction with 259 MeV ^{58}Ni ions accelerated in the Lawrence Berkeley Laboratory SuperHILAC. The beam energy at the center of the target was calculated to be 242 MeV. Products recoiling from the target were mass separated with the OASIS facility[9] on-line at the SuperHILAC. Isobars simultaneously present in the sources included ^{149}Tm, $^{149}Ho^{g+m}$, ^{149}Dy, and $^{149}Tb^{m}$. Sources were collected on a programmable moving tape for fixed intervals of 4, 16, and 160 s and transported to a counting station. A Si particle ΔE-E telescope and a hyperpure Ge detector faced the radioactive layer, while a 1-mm thick plastic scintillator and an n-type Ge detector with a relative efficiency of 52% were located on the other side of the collector tape. In addition, a 24% n-type Ge detector, oriented 90° with respect to the two other Ge detectors, was placed ~4.5 cm from the radioactive source. A schematic diagram of the detector configuration is shown in Fig. 1. Coincidences between particles, γ rays, x rays, and positrons were recorded in an event-by-event mode; all events were tagged with a time signal for half-life determination. Singles were also taken with the x ray and 52% detectors in a multispectrum mode in which the tape cycle was divided into eight equal intervals. All detectors were calibrated for absolute efficiency and energy with standard sources of ^{66}Ga, ^{152}Eu, ^{226}Ra, and ^{241}Am. Analyses of singles data were performed with the γ-ray peak fitting code SAMPO (Ref. 10) and coincidence data were analyzed using software described in Refs. 11–13.

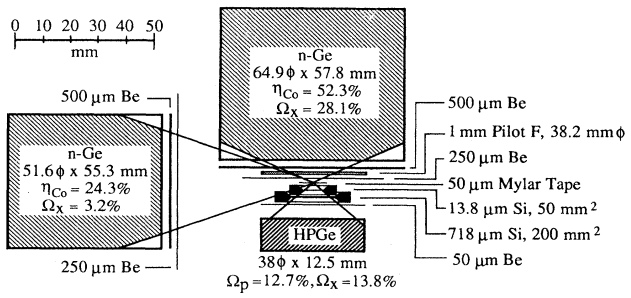

FIG. 1. Arrangement of detectors surrounding the mass separated products collected with the fast cycling tape system at OASIS.

III. EXPERIMENTAL RESULTS

A. γ-ray data

A total of 125 γ rays were assigned to the EC+β^+ decay of $^{149}Er^{g+m}$ and two γ rays previously assigned to $^{149}Er^{m}$ IT decay were confirmed.[8] The γ-ray energies and intensities are listed in Table I. A γ-ray singles spectrum, corresponding to the 16-s data, is shown in Fig. 2. These γ rays were assigned to ^{149}Er on the basis of coincidences with Ho K x rays or other known γ rays and by half-life. Weak transitions were assigned to ^{149}Er decay if they were observed in the 16-s and not the 160-s data and could not be associated with the decay of the longer-lived daughters. In addition, Table I lists the relative intensi-

TABLE I. Transition energies, level assignments, and relative intensities for $^{149}Er^{m+g}$ decay.

E (keV)[a]	Level	I_γ(rel)[bc]	E keV)[a]	Level	I_γ(rel)[bc]	E (keV)[a]	Level	I_γ(rel)[bc]
Ho $K\alpha_2$		137(4)	1605.0(10)	2607.4	~2	2935.7(6)	2935.7	2(1)
Ho $K\alpha_1$		242(5)	1648.9(1)	1648.9	43(5)	2939.3(9)	2939.3	1.3(5)
Ho $K\beta_2$		70(15)	1676.1(4)	2677.3	6(3)	2965.5(3)	2965.5	2(1)
Ho $K\beta_1$		21(2)	1706.9(2)	1706.9	35(4)	2977.8(3)	2977.8	3(1)
106.0(10)[d]	1277.1	~3	1735.3(2)	1735.3	40(4)	2992.3(3)	2992.3	4(2)
111.3(3)[f]	111.3	12(2)	1748.4(1)[i]	1797.4	36(4)	2996.7(3)	2996.7	4(2)
163.1(10)[d]	1765.8	~4	1765.8(1)	1765.8	38(4)	3001.1(4)	3001.1	2(1)
171.5(1)	220.5	76(9)[e]	1824.0(10)	2825.0	~0.5	3005.0(3)	3005.0	3(1)
172.4(10)[d]	1552.1	~3	1828.9(3)	1828.9	7(2)	3049.0(3)	3049.0	5(2)
222.0(10)[d]	1601.9	~6	1913.0(10)	2913.6	~0.8	3061.0(9)	3061.0	0.9(5)
323.8(10)[d]	1601.9	3(1)	1991.0(10)	2992.3	~6	3125.3(3)	3125.3	3(1)
327.1(10)[d]	1706.9	~3	1997.4(3)	1997.5	8(2)	3174.9(5)	3174.9	2(1)
343.9(1)	564.4	69(8)	2000.0(10)	3001.1	~3	3226.2(4)	3226.2	2(1)
359.9(1)	1530.9	8(2)	2004.0(10)	3005.0	~4	3263.1(3)	3263.1	3(1)
380.9(1)	1552.1	7(2)	2071.9(2)	2071.9	3(1)	3305.8(3)	3305.8	1.5(7)
413.0(10)	1415.1	2(1)	2124.0(10)	3125.3	~0.7	3325.2(4)	3325.2	1.0(5)
436.7(1)	1001.2	42(7)	2135.0(5)	2135.0	4(2)	3338.4(3)	3338.4	3(1)
630.5(2)[fe]	741.4	(36)	2148.7(2)	2148.7	6(2)	3536.3(8)	3536.3	2(1)
780.7(1)	1001.2	29(12)	2177.5(1)	2177.5	19(3)	3795.0(6)	3795.1	2(1)
826.4(2)	1997.5	7(2)	2209.0(3)	2209.2	5(2)	3838.2(12)	3828.3	1.0(5)
851.0(5)	1415.1	3(1)	2221.9(1)	2221.9	14(2)	3885.5(5)	3885.6	5(3)
1045.6(10)[d]	2321.7	4(2)	2226.9(2)	2226.9	12(2)	4003.1(4)	4003.2	0.9(4)
1171.0(1)	1171.1	100(10)	2267.2(1)	2267.2	7(2)	4037.2(13)	4037.3	0.3(2)
1183.7(2)	1183.7	6(2)	2297.6(5)	2297.3	4(2)	4086.3(5)	4086.4	2(1)
1194.5(5)	1415.1	6(2)	2317.6(2)	2317.6	16(3)	4235.9(10)	4236.0	0.5(3)
1208.5(5)	2209.2	3(1)	2321.7(1)	2321.7	20(3)	4385.9(7)	4386.0	0.9(5)
1225.8(2)	2226.9	9(3)	2326.8(2)	2326.8	11(4)	4413.4(3)	4413.5	4(2)
1233.0(10)[i]	1797.4	~2	2368.3(2)	2368.3	12(2)	4433.8(4)	4433.9	2(1)
1267.9(5)	2267.2	4(2)	2381.3(2)	2381.3	6(3)	4441.3(3)	4441.4	3(1)
1277.1(1)	1277.1	26(3)	2469.4(2)	2469.3	11(3)	4552.4(8)	4552.5	0.5(2)
1295.0(10)	2297.3	2(1)	2491.9(5)	2492.7	6(3)	4616.7(5)	4616.8	0.8(4)
1320.4(5)	2321.7	6(3)[g]	2499.4(5)	2499.4	3(1)	4622.3(3)	4622.4	4(2)
1367.0(10)	2368.3	~0.8	2512.5(2)	2512.5	8(2)	4645.5(4)	4645.6	2(1)
1380.1(1)	1380.1	34(3)	2580.4(2)	2580.4	6(2)	4652.0(4)	4652.1	2(1)
1448.8(5)	2450.0	8(4)	2591.4(4)	2591.4	5(2)	4661.6(2)	4661.7	4(2)
1468.1(5)	2469.3	14(7)	2607.4(1)	2607.4	15(3)	4676.6(4)	4676.7	2(1)
1492.3(5)	2492.7	4(2)	2633.3(4)	2633.3	2(1)	469.6(2)	4699.7	15(3)
1530.9(1)	1530.9	47(5)	2714.8(3)	2714.8	4(2)	4706.0(10)[d]	4706.1	1.2(6)
1552.2(1)	1552.1	19(3)	2804.5(5)	2804.5	1.0(5)	4749.9(8)	4750.0	1.1(5)
1560.1(1)	1560.1	32(3)	2824.9(4)	2824.9	7(2)	4822.8(6)	4851.1	0.7(4)
1577.9(3)[i]	1797.4	10(3)	2851.2(11)	2851.2	3(1)	4851.0(9)	4851.1	0.7(4)
1581.6(2)	2996.7	7(3)	2901.7(4)	2901.7	2(1)	5079.1(10)[d]	5079.2	~1.3
1602.0(10)	1602.0	12(4)	2913.5(3)	2913.6	3(1)	5098.6(10)[d]	5098.7	~1.3

[a]Assigned to $^{149}Er^{m}$ decay except where noted.
[b]Intensity relative to $I_\gamma(1171.0)=100$. For the x rays, an additional systematic uncertainty of 15% should be added.
[c]For absolute intensity per 100 decays of $^{149}Er^{m}$, multiply by 0.097(20).
[d]Only observed in coincidence; intensity derived from coincidence data.
[e]Includes $I_\gamma=7(3)$ from $^{149}Er^{g}$ decay.
[f]From $^{149}Er^{m}$ IT decay.
[g]Also observed with ^{149}Ho decay; intensity suitable divided.
[h]Transition partially obscured by an impurity.
[i]Transition assigned to $^{149}Er^{g}$ decay; for absolute intensity per 100 decays multiply by 2.0(2).

ties of Ho K x rays observed in the hyperpure Ge detector. From the decay scheme and these data, we derived the relative intensities $I(\mathrm{EC})=510\pm140$ and $I(\beta^+)=550\pm140$ with respect to $I_\gamma(1171\ \mathrm{keV})=100$. The total electron-capture intensity was calculated from the Ho K x-ray intensity assuming a 7.4% contribution from internal conversion. The fluorescence yield was taken as $\omega_k=0.943$,[14] and $I_{\mathrm{EC}(K)}/I_{\mathrm{EC(tot)}}=0.835$.[15] The total β^+ decay intensity was calculated from the $\gamma^{\pm}(511\ \mathrm{keV})$ intensity corrected annihilation-in-flight.[16] The annihilation intensity associated with $^{149}Er^{g+m}$ decay was derived from a multicomponent half-life analysis of the annihilation peak. The absolute normalization of γ-ray intensities was calculated from the measured $\mathrm{EC}+\beta^+$ intensity which was apportioned between $^{149}Er^m$ and $^{149}Er^g$ decays as described in Sec. IV. Coincidences between all three Ge detectors were analyzed and are summarized in Table II; a γ-ray spectrum in coincidence with the 171.5-keV is shown in Fig. 3. Conversion electrons were not measured; however, K conversion coefficients for the strong, more converted transitions were calculated from the summing intensity for Ho K x rays with γ rays. For the $^{149}Er^m$ IT transitions, the K conversion coefficients were derived from sum intensities in the singles spectrum, and for transitions in ^{149}Ho, they were derived from sum intensities in the Ho K x-ray coincident gate, neglecting the

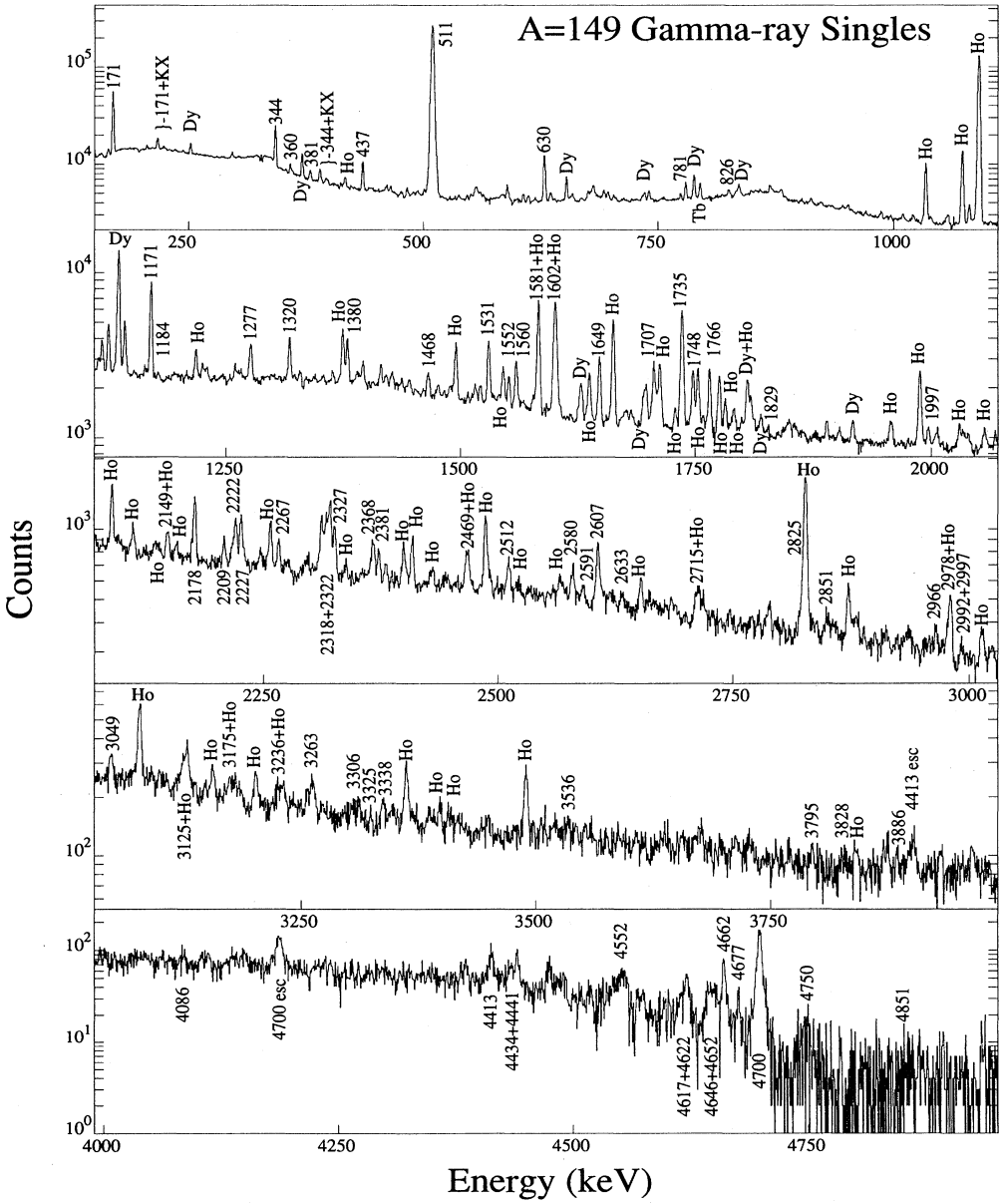

FIG. 2. Gamma-ray singles spectrum taken with the 52% Ge detector during the 16-s tape cycle. Background, counted after the experiment, has been subtracted. The spectrum is plotted in 0.64 keV per channel intervals.

TABLE II. $\gamma\gamma$ coincidence results.

Gate	Coincident γ rays
Ho K x rays	172,(324),327,344,360,381,413,437 781,826,851,1171,1184,1194,1208 1268,1277,1320,1367,1380,1448,1468 1531,1552,1560,1578,1582,1602,1649 1676,1707,1735,1748,1766,(1824),1829 1997,2072,2149,2178,2209,2222,2227 2267,2298,2318,2322,2327,2381,2469 2513,2580,2591,2607,2633,2715,2936 2966,2978,2992,2997,3005,3049,4413 4441,4652,4662,4700,4706,5079,5099
Er K x rays	111,630
111	630
172	344,437,781,851,1194,1208,1226,1268 1295,1320,1448,1468,1492,1577,1582 1605,1676,1824,1913,1991,2124,(2135)
344	171,413,437,781,851,1194,1208,1226 1233,1268,1448,1468,1492,1605,1676 1991,2004
437	171,344,413,1226,1295,1320,1448,1468 1492,1582,1605,1991,2000,2004
630	111
781	171
1171	106,360,381,826
1277	324,1046
1380	172,222,327
1602	163,(171,344,427)

contribution from high-energy transitions. These results are summarized in Table III.

B. Proton data

Proton events were identified with the Si particle ΔE-E telescope. Spectra of all protons and the protons in coincidence with positrons are shown in Fig. 4. The total proton spectrum can be characterized as narrow peaks superimposed on a continuous distribution. These peaks were not wider than the experimental resolution ($\sim$35 keV FWHM), but we cannot rule out the possibility that some peaks may represent close lying multiplets. The

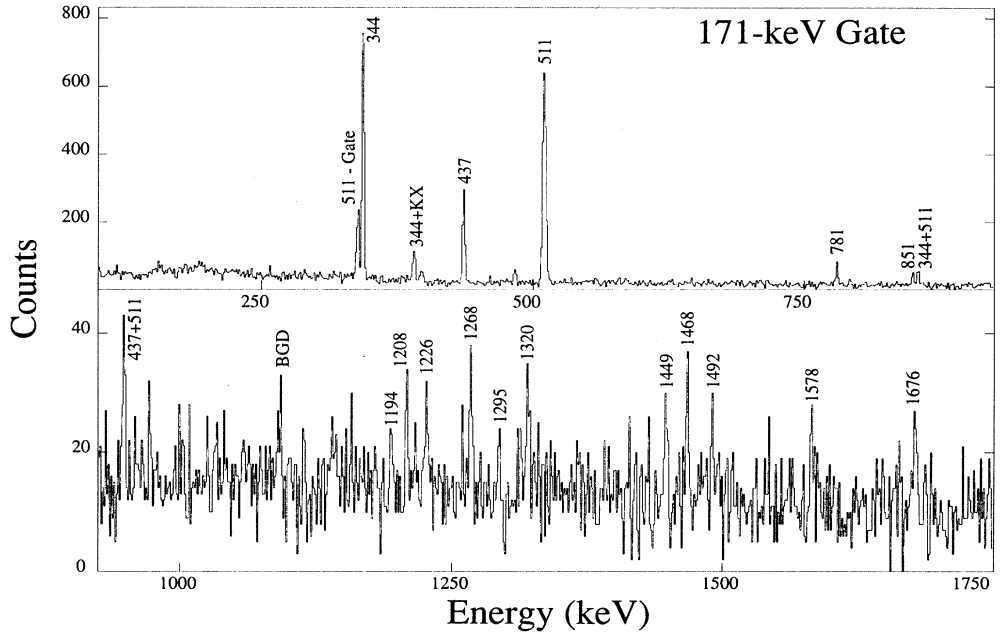

FIG. 3. Gamma rays in coincidence with the 171.5-keV gate. The gate was set in the HPGe detector and coincidences for all tape cycles are displayed in the 52% Ge detector. The spectrum is plotted in 1.3 keV per channel intervals.

TABLE III. Experimental and theoretical conversion coefficients.

		α_K (theory)						
E_γ	α_k(expt.)	$E1$	$E2$	$M1$	$M2$	$M3$	$M4$	Adopted multipolarity
111.3	1.82±0.11	0.20	0.82	1.82	13.6	63.1	268	$M1$
171.5	0.57±0.07	0.064	0.252	0.492	2.75	11.8	48.8	$M1$
343.9	0.14±0.03[b]	0.011	0.034	0.074	0.272	0.841	2.56	$M1$
436.7		0.006	0.018	0.040	0.130	0.357	0.965	$M1$
630.5	0.27±0.03	0.003	0.008	0.017	0.047	0.110	0.248	$M4$

[a]F. Rosel, H. M. Fries, K. Alder, and H. C. Pauli, At. Data Nucl. Data Tables **21**, 91 (1978).
[b]From the 171.5+Ho K x-ray sum peak in the Ho K x-ray coincidence gate. The sum of the K conversion coefficients is most consistent with both transitions assigned as $M1$.

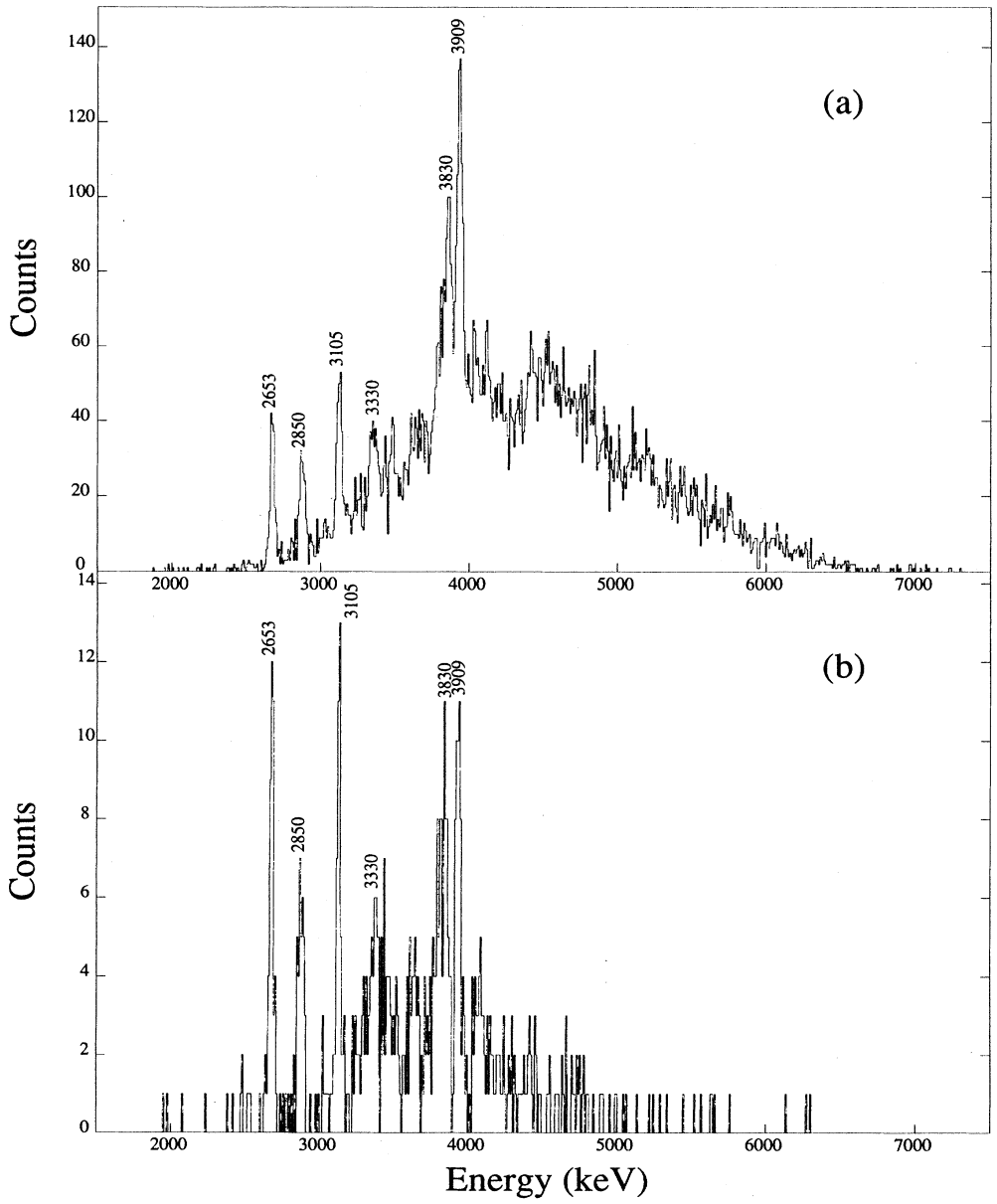

FIG. 4. Beta-delayed proton spectrum (a) and protons in coincidence with positrons (b). Positron coincidences were defined by an event in the 1-mm plastic scintillator. The spectrum is plotted in 9.2 keV per channel intervals.

resolved proton peak energies are shown in Fig. 4 and the intensities in Fig. 5. The positron coincident proton spectrum also has the pronounced structure, but the continuous component is strongly suppressed. We interpret this result as indicating that the structured proton decay arises from levels where the β-decay energy is high and the level density is low, while the continuous proton spectrum is presumed to arise mainly from levels with lower β-decay energies where the level density is too high to resolve individual transitions. Several γ rays in ^{148}Dy were observed in coincidence with the protons and are summarized in Fig. 5. The intensity of the protons from $^{149}Er^{g+m}$ was 5.2 ± 0.6 relative to $I(1171\ \text{keV})=100$. From the coincidence and singles proton intensities, we determine that for delayed proton decay the total $EC/\beta^+=0.83\pm0.04$.

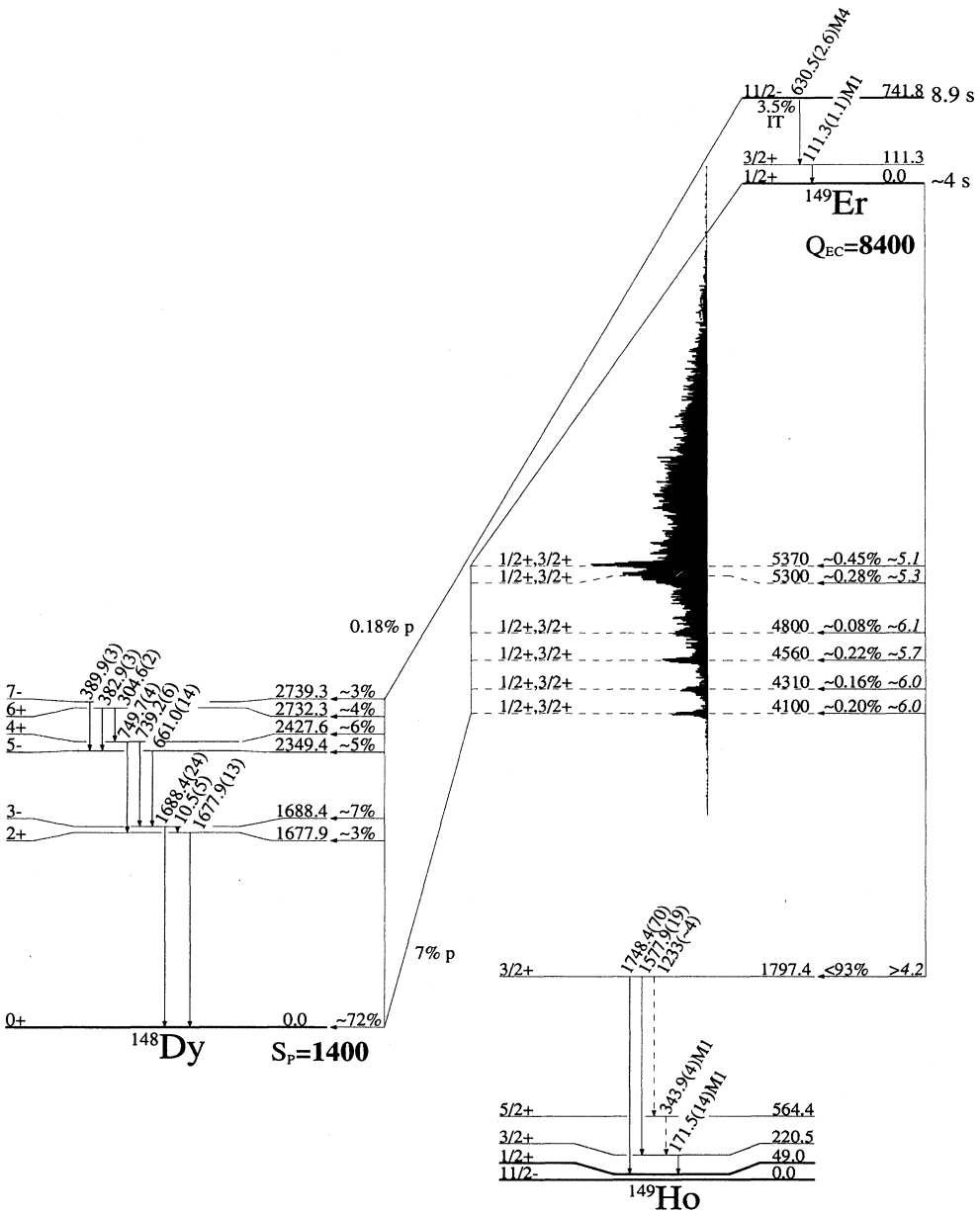

FIG. 5. Beta-delayed proton decay schemes for $^{149}Er^{m+g}$ and decay schemes for $^{149}Er^{m}$ IT decay and $^{149}Er^{g}$ electron capture/positron decay. The γ-ray energies in ^{148}Dy are taken from Toth, Sousa, Nitschke, and Wilmarth, Phys. Rev. C **37**, 1198 (1988), and the intensities are given per 100 proton decays. The intensities shown for $^{149}Er^{m}$ IT decay and $^{149}Er^{g}$ EC+β^+ decay are shown on an absolute scale. The spectrum of proton energies is overlaid, to scale, on the ^{149}Ho level diagram. Level energies corresponding to the proton group energies have been recoil corrected and were calculated assuming $S_p=1.4$ MeV. The beta feedings to the proton groups reflect only the proton intensity and are not corrected for gamma-ray deexcitation.

C. Half-life determination

The half-life of $^{149}Er^{m}$ was determined by following the decay of the stronger γ rays during the 16-s tape cycle. A constant-rate pulser peak was included in the spectrum for dead-time correction which proved negligible. The half-life data points were fit by a least-squares procedure with a single component using the computer code CLSQ.[17] From an analysis of the strongest γ-ray transitions, we have adopted a weighted average half-life for $^{149}Er^{m}$ of 8.9 ± 0.2 s. This value is lower than the previous value of 10.8 ± 0.6 s of Schardt *et al.*,[7] but is consistent with 9 ± 1 s from Toth *et al.*[6] The half-life of $^{149}Er^{g}$ could not be determined directly because it was produced weakly in the reaction and decayed in approximate equilibrium with $^{149}Er^{m}$ decay. We have shown in Sec. IV that $(63\pm7)\%$ of the protons were from $^{149}Er^{g}$ decay. Analysis of the growth and decay of the 16-s proton data is consistent with $t_{1/2}<8$ s for $^{149}Er^{g}$. The half-life of $^{151}Yb^{g}$ is 1.6 ± 0.1 s (Ref. 5) which should be systematically lower than the $^{149}Er^{g}$ half-life. From the $^{149}Er^{g}$ decay scheme, described in Sec. IV, assuming equilibrium with $^{149}Er^{m}$ IT decay, a half-life of 4 ± 2 s is obtained. This value is consistent with both limits and has been adopted for the following discussion.

D. Determination of Q_{EC}

The Q_{EC} values for $^{149}Er^{g+m}$ decays have been determined in two ways. From the intensity of x rays and annihilation in coincidence with the 4699.6-keV transitions, assuming negligible feeding from higher-lying levels, we determine that $EC/\beta^{+}=0.68\pm0.34$ to the 4.7-MeV level deexcited by that transition (see Sec. IV). This corresponds to a decay energy of $4.4^{+0.9}_{-0.4}$ MeV (Ref. 15) to that level and a total $Q_{EC}=9.1^{+0.9}_{-0.4}$ MeV. Alternatively, the value of $(Q_{EC}-S_p)$ can be calculated from the ratio of intensities in the total and positron-coincident proton spectra. This ratio is proportional to $(EC+\beta^{+})/\beta^{+}$. The 2653-, 2850-, 3105-, and 3909-keV proton groups were analyzed by a χ^2 analysis where

$$\chi^2=\sum_i \frac{(R_{exp}-R_{th})^2}{\Delta R^2_{exp}} ,$$

where R_{exp} and R_{th} are the experimental and theoretical $(EC+\beta^{+})/\beta^{+}$ ratios for each proton group. The χ^2 minimization of the decay energy is shown in Fig. 6 from which we determine with a 90% confidence limit that $(Q_{EC}-S_p)=7.0^{+0.5}_{-0.4}$ MeV. from Wapstra *et al.*[18] systematics, $S_p=1.17\pm0.21$ MeV, implying $Q_{EC}=8.2\pm0.5$ MeV. This value is consistent with the first value, if we assume that the proton groups are associated with $^{149}Er^{g}$ decay and the 4699.6-keV γ ray with $^{149}Er^{m}$ decay. From these two measurements and the $^{149}Er^{m}$ excitation energy of 0.74 MeV, we determine that $S_p=1.4^{+1.0}_{-0.6}$ MeV, which is consistent with the value from systematics.[18] For the following discussion we have adopted $Q_{EC}=8.4^{+0.9}_{-0.4}$ MeV for $^{149}Er^{g}$ decay. This value is comparable to 8.65 MeV calculated from the masses of Liran and Zeldes[19] which are generally reliable in this mass region.

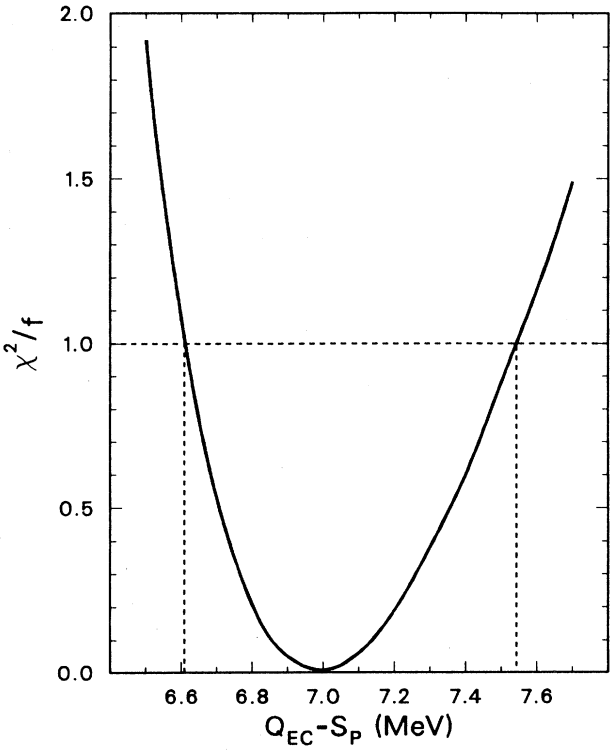

FIG. 6. Fit to $Q_{EC}-S_p$ for decay to levels associated with structured proton decay. The experimental $\beta^{+}/(\beta^{+}+EC)$ is compared to the theoretical ratio for various $Q_{EC}-S_p$ values plotted on the abscissa.

IV. DECAY SCHEMES

The decay scheme for $^{149}Er^{m}$ is shown in Fig. 7. This scheme was constructed on the basis of coincidence data and intensity balances. The transitions deexciting the levels at 220.5, 564.4, and 1001.2 keV were previously reported by Toth *et al.*[8] and are confirmed here. We also observe a new 780.7-keV transition from the 1001.2-keV level. A possible transition deexciting the 564.4-keV level to the 49.0-keV state would be overwhelmed by the intense annihilation peak. No 563-keV Ho K_α sum peak is observed in the 52% detector so we have set an upper limit on the 515.4-keV γ-ray intensity of 12% of the 1171.0-keV γ-ray intensity. The excitation energy of the $\frac{1}{2}^{+}$ isomer in ^{149}Ho with respect to the $\frac{11}{2}^{-}$ ground state was determined as 49.0 ± 0.1 keV. This is established by coincidences between the 171.5-, 343.9-, and 436.7-keV γ rays with transitions of 1208.5, 1225.8, 1267.9, 1320.4, 1468.1, and 1492.3 keV. The coincident transitions deexcite levels that also directly populate the $\frac{11}{2}^{-}$ ground state and determine the energy of the $\frac{7}{2}^{+}$ state at 1001.2 keV. Additional weak transitions feeding the 1001.2-keV level were similarly placed on the basis of energy sums. Levels deexcited by this pattern are restricted to having $J^{\pi}=\frac{9}{2}^{-}$ if they are directly fed by beta decay. Transitions deexciting levels which decay only to the ground state could not be uniquely assigned to $^{149}Er^{m}$ decay. However, assignment to $^{149}Er^{g}$ decay is unlikely due to

the nearly saturated intensity balance in that decay (see below) and the probability that low-spin levels would also deexcite through the 220.5- and 564.4-keV levels.

The isomer $^{149}Er^m$ decays by both IT and EC+β^+ modes. The IT decay proceeds via a 630.5($M4$) $\rightarrow$111.3($M1$) cascade analogous to the lighter $N=81$, odd-A isotones. The IT decay scheme is shown in Fig. 5. We have chosen to normalize the IT branch to the 111.3-keV transition intensity because the 630.5-keV transition is partially obscured by an impurity from ^{149}Ho decay. To obtain the relative intensity of the $^{149}Er^m$ EC+β^+ decay branch, the total observed EC+β^+ feeding must be corrected for the $^{149}Er^g$ contribution. Assuming that the ground-state decay is in approximate equilibrium with the IT decay, and the 111.3-keV γ ray is $M1$ ($\alpha_{tot}=1.99$), we determine that (4.8±1.0)% of the total observed EC+β^+ decay is associated with $^{149}Er^g$ decay, and $^{149}Er^m$ decays by IT (3.5±0.7)% and EC+β^+ (96.5±0.7)%. The beta feedings in Fig. 7 are calculated from intensity balances and are presumed to be upper limits due to unobserved additional γ-ray feedings from higher levels. About 89% of the $^{149}Er^m$ decay intensity can be accounted for by the IT decay and the observed ^{149}Ho ground-state γ-ray feeding. The remaining 11% unplaced intensity can be divided between unobserved beta feeding to the ground state and to the continuum of levels above 5 MeV where proton emission is observed. For $^{147}Dy^m$ decay,[20] the analog transition has log$ft>6.5$. Assuming this value, we expect <5% feeding to the ground state with the remainder feeding higher levels.

From the γp coincidence data we propose the β-delayed proton decay scheme for $^{149}Er^m$ in Fig. 5. Proton decay from $^{149}Er^m$ is hindered to the 0^+ ground state of ^{148}Dy by the angular momentum mismatch. Less hindered channels for proton decay to excited states in ^{148}Dy do not open until nearly 2 MeV above S_p. Conversely, proton decay from $^{149}Er^g$ to the ^{148}Dy ground state is not expected to be hindered, while population of the 2^+ level at 1.7 MeV in ^{148}Dy should not compete strongly due to the additional excitation energy. We have performed sta-

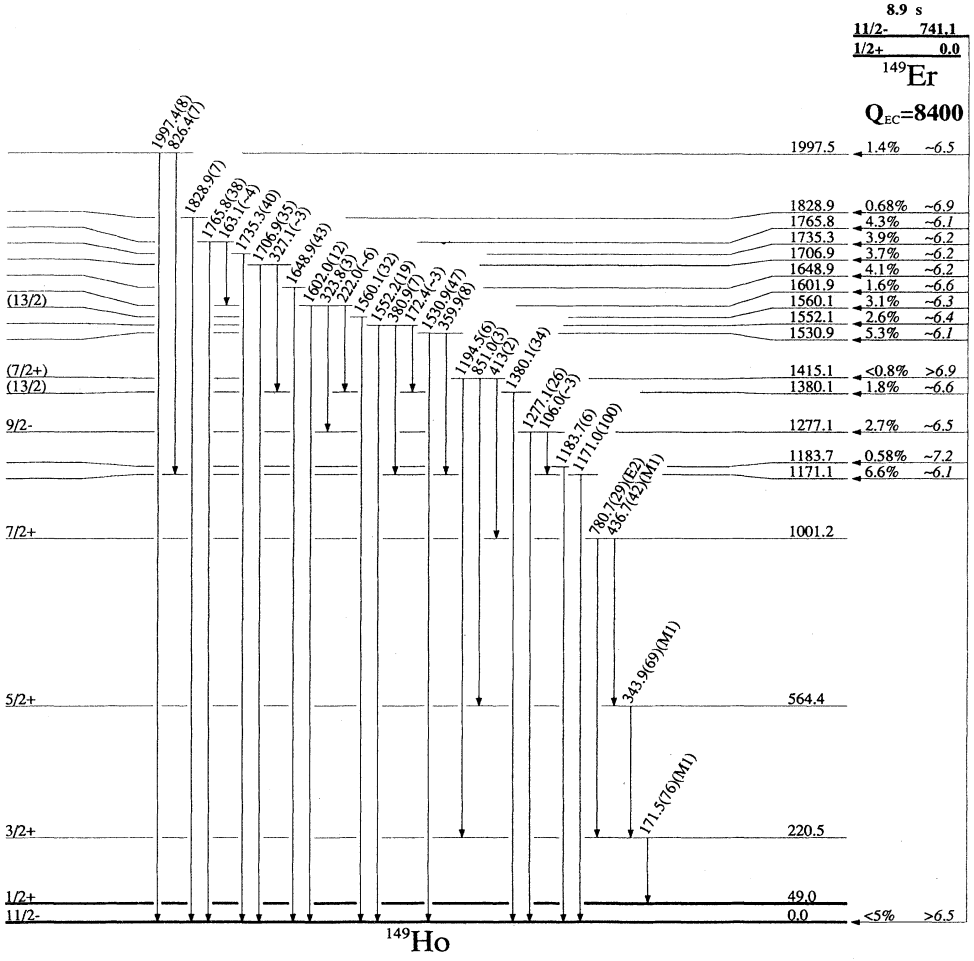

FIG. 7. Decay scheme for $^{149}Er^m$ decay. The level energies are calculated from a least-squares fit of the recoil corrected γ-ray energies to the level scheme.

tistical model calculations[21] which predict about 24% of the $^{149}Er^{m}$ delayed-proton decay to the ^{148}Dy ground state and less than 1% of the $^{149}Er^{g}$ decay to the 2^{+} level. Assuming the statistical model value for the ground-state feeding from $^{149}Er^{m}$, with an uncertainty of 10% in that branching intensity, and that all of the ^{148}Dy excited state feeding is associated with $^{149}Er^{m}$ decay, we determine that $(37\pm7)\%$ of the observed protons are associated with $^{149}Er^{m}$ decay. From this proton intensity we determine a $(0.18\pm0.07)\%$ β-delayed proton branch for $^{149}Er^{m}$ decay.

A decay scheme for $^{149}Er^{g}$ is given in Fig. 5. A level at 1797.4 keV has also been associated with the decay of $^{149}Er^{g}$ on the basis of coincidence between the 171.5-keV γ ray and the 1233- and 1577.9-keV γ rays, and the observation of an intense 1748.4-keV transition that is coincident with Ho K x rays. Nearly all of the beta feeding from $^{149}Er^{g}$ decay appears to go to the 1797.4-keV level, although its low $\log ft$ probably indicates unobserved γ-ray feeding from higher levels. The intensity through the 220.4-keV level is nearly balanced, suggesting that no other levels are strongly fed. From the systematics of the lighter $N=81$ odd-A decays, we expect little feeding to the 49.0- or 220.4-keV levels. The decay scheme has been normalized to the sum of the transition intensities deexciting the 1797.4-keV level and the proton intensity apportioned to $^{149}Er^{g}$ decay. As described in the preceding paragraph, $(63\pm7)\%$ of the β-delayed protons are associated with $^{149}Er^{g}$ decay. This corresponds to a $(7\pm2)\%$ proton branch. Nealy 20% of the β-delayed protons assigned to the decay of $^{149}Er^{g}$ are associated with resolved proton groups. The remainder are in the continuous proton spectrum which deexcite levels up to over 8 MeV in ^{149}Ho. In Fig. 5, the proton decaying group excitation

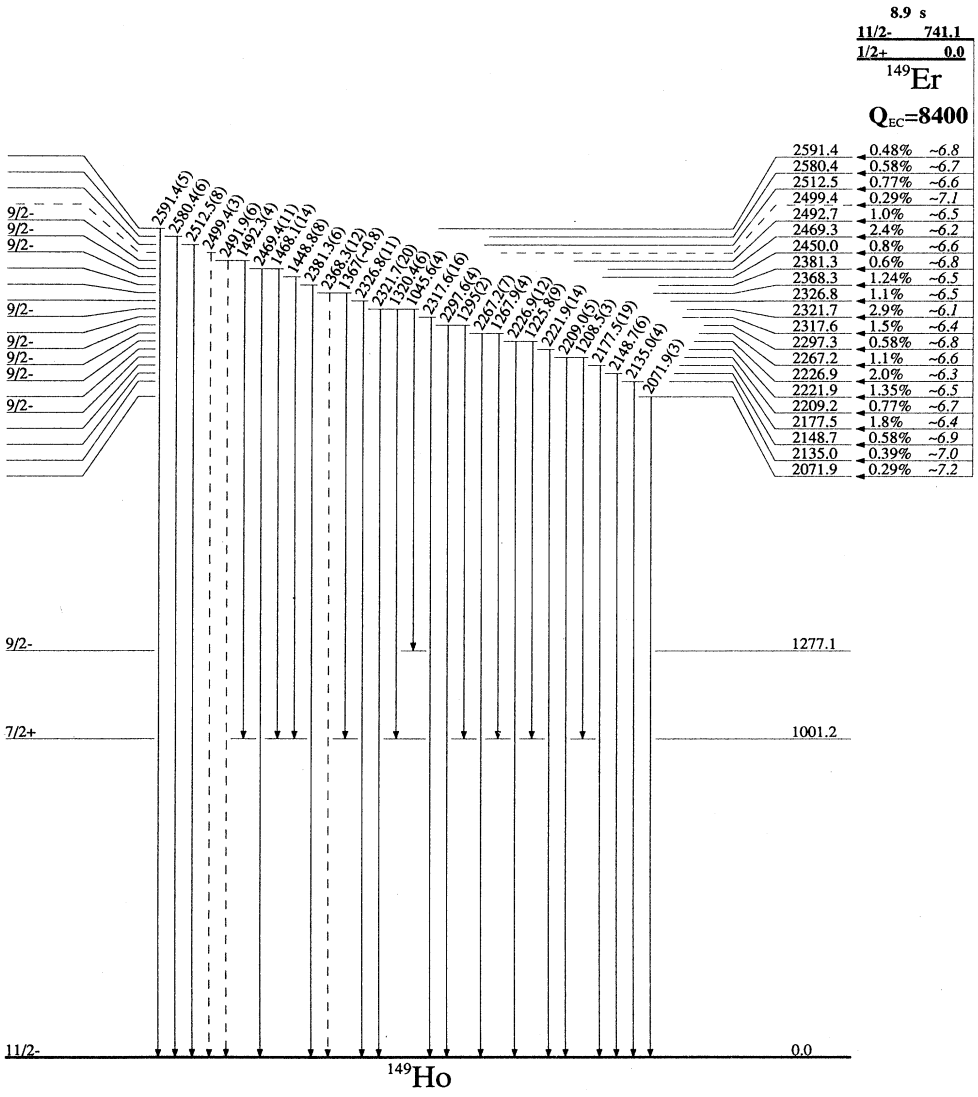

FIG. 7. (*Continued*).

energies are calculated from the measured energies assuming $S_p = 1.4$ MeV. The statistical model[21] predicts that Γ_γ/Γ_p should vary from 5000 to 50 for levels at 4–5 MeV in ^{149}Ho. The limit for detecting a γ ray of 4–5 MeV is about 6% per ^{149}Er^g decay and no γ-ray deexcitation from the proton emitting levels was identified. This is consistent with Γ_γ/Γ_p varying from <30 for the 4100-keV level to <13 for the 5370-keV level. The intensity is nearly balanced through the $\frac{3}{2}^+$ level in ^{149}Ho indicating that there is little direct γ-ray depopulation of the proton emitting levels. We conclude that Γ_γ is much smaller than predicted because proton emission is a simple process which is not expected to be significantly hindered.

V. DISCUSSION

A. Electron capture/positron decay

The level structure in ^{149}Ho can be described by a simple weak-coupling plus shell-model description analogous to that of ^{145}Eu.[1] In this description, the low-lying levels of ^{149}Ho are assumed to be single-particle shell-model states, and levels at higher excitations are explained by weak coupling of levels in the even-even ^{148}Dy core with these single-particle states. The residual interactions are assumed to be small so that the individual couplings cluster around the energy of the core plus single-particle states. The $\pi h_{11/2}$, $\pi s_{1/2}$, $\pi d_{3/2}$, $\pi d_{5/2}$, and $\pi g_{7/2}$ single-particle shell-model proton states are at 0, 49.0,

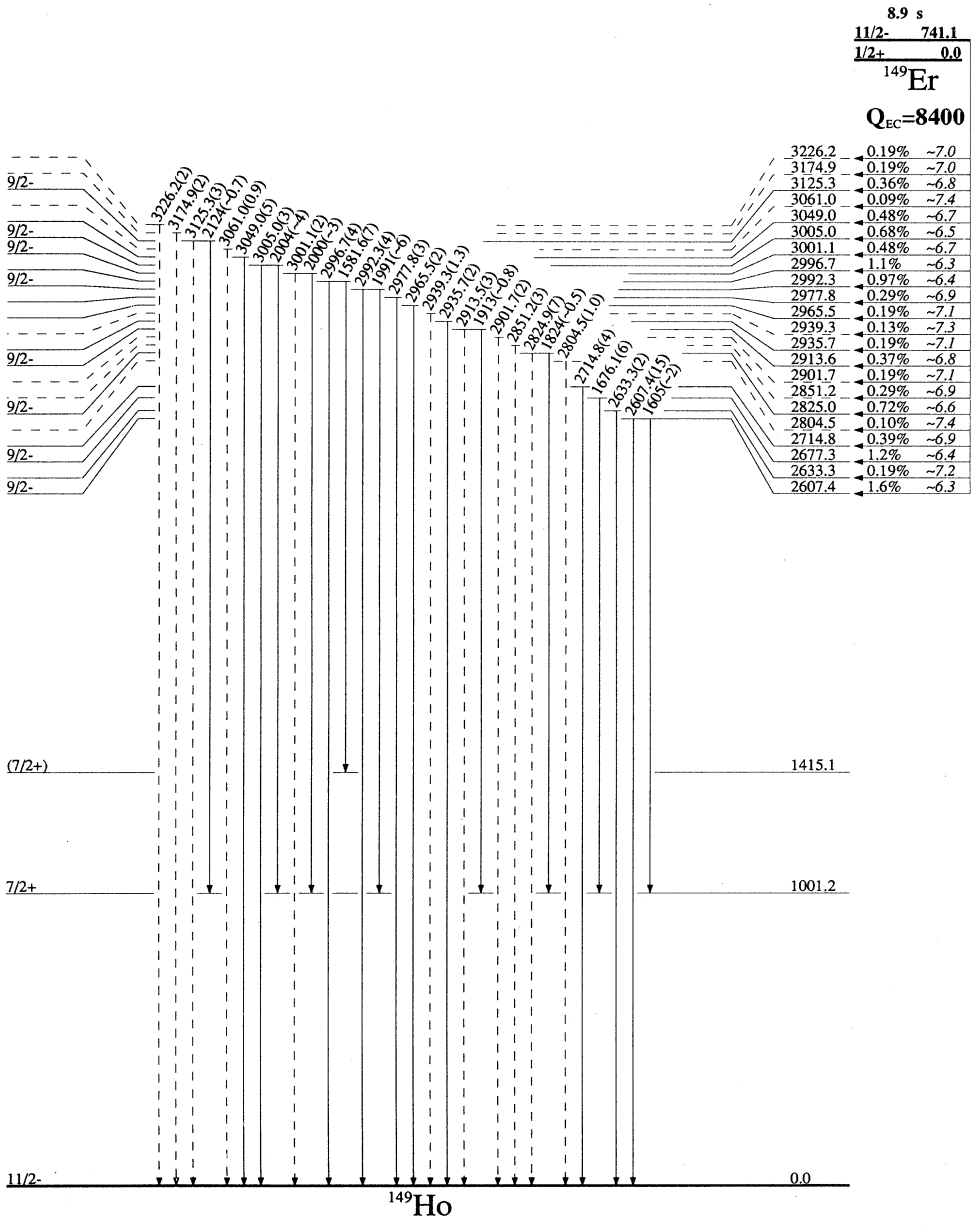

FIG. 7. (*Continued*).

220.5, 564.4, and 1001.2 keV. For $^{149}Er^{m}$ decay, the allowed EC+β^+ transition $(\pi h_{11/2})^4(\nu h_{11/2})^{-1} \rightarrow (\nu h_{11/2})^3$ is very hindered. The analogous logft values for $^{147}Dy^{m}$ (Ref. 20) and $^{145}Gd^{m}$ decays[2] are >6.5 and >7.4, respectively. These allowed transitions are hindered, in part, due to the nearly full $\nu h_{11/2}$ orbital.

Levels between 1.2 and 3.5 MeV can be described by weak coupling of the single-particle shell-model states to levels in the ^{148}Dy core. For decay to these levels, the odd particle acts as a spectator so the decay is analogous to that of ^{148}Ho to the core. This is illustrated in Table IV, where simplified decay data for the $N=81$ odd-A nuclei and their core nuclei are compared. For $^{149}Er^{m}$ and ^{148}Ho the decays populate two level groupings near 1.6 MeV (2^+, 3^-) and 2.6 MeV (4^+, 5^-, 6^+, 7^-). The experimental logft values and resonance energies are similar for both decays consistent with the weak-coupling description. The energies of the ^{149}Ho groups are both

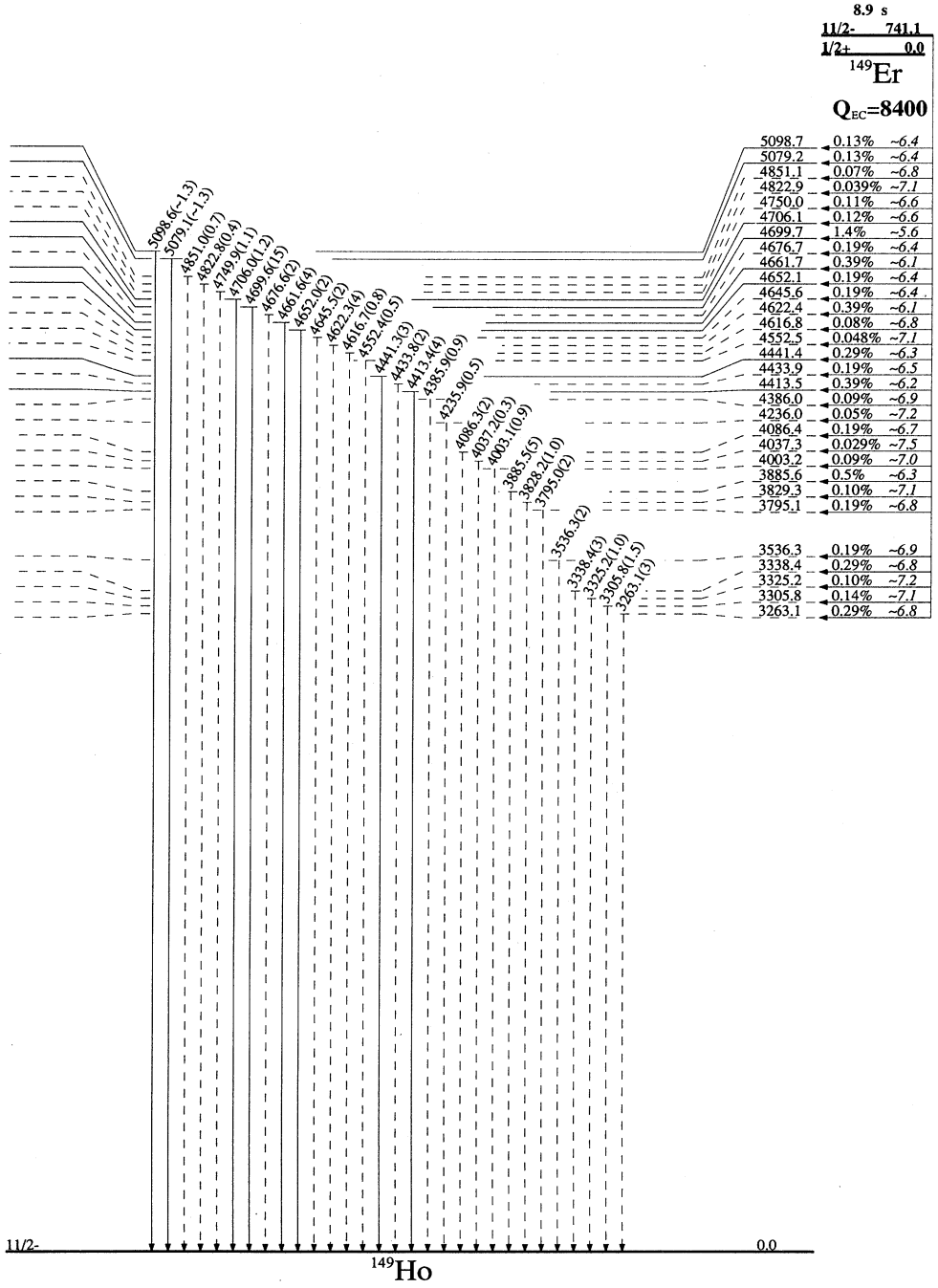

FIG. 7. (*Continued*).

TABLE IV. Systematics of $N=81$ beta decays.

	Dominant core configuration[a]					
	$2^+,3^-$		$4^+,5^-,6^+,7^-$		$(\nu h_{9/2})$	
Transition	E_x[b]	logft	E_x[b]	logft	E_x[b]	logft
$^{149}Er^m \rightarrow {}^{149}$Ho	1523	5.2	2498	5.0	4530	4.4
$^{149}Er^g \rightarrow {}^{149}$Ho	1797	>4.2			4700	4.2
$^{148}Ho^{g+m} \rightarrow {}^{148}$Dy	1682	~ 5.5	2653	~ 4.9	4300	<5.1
$^{147}Dy^m \rightarrow {}^{147}$Tb	1482	5.2	2260	4.9	4800	3.9
$^{147}Dy^g \rightarrow {}^{147}$Tb	1763	5.0			4100	~ 3.7
$^{146}Tb^{g+m} \rightarrow {}^{146}$Gd	1971	~ 5.4	2841	4.6	4730	4.5
$^{145}Gd^g \rightarrow {}^{145}$Eu	1819	5.4			4500	4.4
$^{144}Eu^{g+m} \rightarrow {}^{144}$Sm	1660	4.9	2450	5.1		

[a]Core configuration that is coupled to the $\pi s_{1/2}$ or the $\pi h_{11/2}$ odd proton in the daughter nucleus.
[b]Intensity weighted average excitation energy of the core-coupled configurations populated by beta decay.

about 160 keV lower than the ^{148}Dy groups. This probably represents the average residual interaction for the $\frac{9}{2}^-$, $\frac{11}{2}^-$ and $\frac{13}{2}^-$ couplings. A one-to-one correspondence between weak-coupled states and experimentally observed levels is impractical due to the large number of possible couplings. However, nine levels with $J^\pi=\frac{9}{2}^-$, $\frac{11}{2}^-$, $\frac{13}{2}^-$ and six levels with $J^\pi=\frac{9}{2}^+$, $\frac{11}{2}^+$, $\frac{13}{2}^+$ between 1–2 MeV are expected. Fifteen levels are observed in that region. Wilson *et al.*[22] have reported levels in ^{149}Ho at 1380 and 1560 keV to which they assigned J^π values of $(\frac{15}{2}^+)$ and $(\frac{15}{2}^-)$, respectively. These levels appear to be too strongly populated by decay to have such high spins; however, observation in a heavy-ion reaction is probably consistent with $J=\frac{13}{2}$ for both levels. In addition, only one level near 1.75 MeV with $J^\pi \leq \frac{3}{2}^+$ is expected. That level can be represented by the $\frac{3}{2}^+$ component of the $(\pi s_{1/2})^1 \times 2^+$ configuration and is probably the 1797.4-keV level populated by $^{149}Er^g$ decay. Similar configurations near 1.8 MeV are strongly populated by $^{145}Gd^g$ and $^{147}Dy^g$ (Ref. 7) decays, and are summarized in Table IV.

Between 3.8 and 5.1 MeV of excitation in ^{149}Ho, 25 levels were populated by $^{149}Er^m$ decay with logft values as low as 5.6. About 11% of the total beta decay was placed to this region with an aggregate log$ft \sim 4.8$. This large transition strength is associated with the $\pi h_{11/2} \rightarrow \nu h_{9/2}$ spin-flip transition. The splitting of this transition strength among many levels can be explained, in part, by the 27 possible couplings of the resulting $\pi h_{11/2} \nu h_{9/2} (\nu h_{11/2})^{-1}$ three quasiparticle configurations leading to $J^\pi=\frac{9}{2}^-$, $\frac{11}{2}^-$, $\frac{13}{2}^-$ and also by configuration mixing. Similar structure has been observed by Alkhazov *et al.*[20] in the decay of $^{147}Dy^{g+m}$ where log$ft=3.9$ to the region near 4.8 MeV in ^{147}Tb. An analogous $\pi h_{11/2} \rightarrow \nu h_{9/2}$ transition has been observed in $^{149}Tb^m$ decay[23] with a log$ft=4.3$. Six level groups from 4.1–5.4 MeV were observed with $^{149}Er^g$ decay. This decay should also be dominated by the $\pi h_{11/2} \rightarrow \nu h_{9/2}$ spin-flip transition. In this case $(\pi h_{11/2})^3 (\nu h_{9/2})^1 \nu s_{1/2}$ three quasiparticle configurations are populated. Three $\frac{1}{2}^+$, $\frac{3}{2}^+$ states can be constructed from this configuration, and 21 additional three-quasiparticle states can be constructed if the third particle is $\nu d_{3/2}$, $\nu d_{5/2}$, or $\nu g_{7/2}$. From the proton decay intensity to this region we infer a log$ft \sim 4.2$, which is comparable to $^{145}Gd^g$ (Ref. 24) and $^{147}Dy^g$ (Ref. 7) decays summarized in Table IV.

About 11% excess decay intensity remains, which probably populates levels at high excitation energies in ^{149}Ho. This intensity is apparently divided among many levels because no resolved high-energy γ rays were observed. If we assume that this decay populates an average level at 5 MeV, we obtain an effective log$ft=4.5$. This strength combined with the resolved feeding to levels below 5 MeV in ^{149}Ho is comparable to that observed in $^{147}Dy^m$ decay. It is remarkable that both the $\frac{1}{2}^+$ and $\frac{11}{2}^-$ $N=81$ odd-A decays populate the region near 4.8 MeV in the daughter with log$ft \sim 4$. This confirms that the $\pi h_{11/2} \rightarrow \nu h_{9/2}$ transition is dominant in both decays with the odd neutron acting as a spectator. Similar beta strength to high excitation in the daughter can also be inferred from the delayed proton spectra of the odd-odd $N=81$ nuclei ^{148}Ho, ^{150}Tm, and ^{152}Lu.[25] In these odd-odd decays, separate $\pi h_{11/2} \rightarrow \nu h_{9/2}$ spin-flip transitions are possible, corresponding to decay of either an odd proton or a paired proton. The former transition populates two-quasiparticle levels analogous to those described in the preceding paragraph, and the latter transition leads to a four-quasiparticle configuration which lies about 2 MeV higher. Because only a single $\pi h_{11/2}$ proton can decay to the lower configuration while several paired protons can decay to the higher configuration, the transition probability to the higher configuration is expected to be larger. The number of possible couplings in the four-quasiparticle configuration is so large that no single configuration would be expected to carry sufficient strength to be experimentally resolved. The situation in the odd-A $N=81$ isotones is different because our simple picture assumes that all protons are paired. Decay to the three-quasiparticle configuration might be expected to dominate because the higher five-quasiparticle states require the breaking of two $\pi h_{11/2}$ pairs. If, however, we assume that the $\pi h_{11/2}$ proton pairs are strongly coupled, then the higher seniority final-state configurations can be readily populated. This would explain the significant beta strength to levels above ~ 6 MeV inferred from the

delayed proton decay. Similar couplings have been described for $f_{7/2}$ shell nuclei.[26–28] For $^{147}Dy^{m}$ decay, Alkhazov *et al.*[20] have observed nearly constant beta strength, with $\log ft \sim 4.6$ to the region from 5.4 to 6.6 MeV in ^{147}Tb. Decay to this higher excitation region is probably dominated by the five-quasiparticle structure.

B. Delayed proton decay

The proton spectra from $^{149}Er^{g}$ and $^{149}Er^{m}$ are markedly different. This difference arises for two principal reasons. First, the energetics of the two decays are not the same. Levels populated by allowed Gamow-Teller $^{149}Er^{g}$ beta decay can deexcite via $L=0$ proton decays to the ground state of ^{148}Dy. Thus, proton emission becomes important near 4.0 MeV of excitation in ^{149}Ho. Conversely, $L=0$ proton emission from levels fed by $^{149}Er^{m}$ beta decay populates levels near 2 MeV in ^{148}Dy, and $L \geq 4$ is required for the transition to the ground state of ^{148}Dy. In this case, proton emission does not become significant until higher excitation energies in ^{149}Ho. Second, the proton emitting levels near 4 MeV in ^{149}Ho, populated by $^{149}Er^{g}$ decay, have much smaller γ-ray widths than the comparable levels populated by $^{149}Er^{m}$ decay. The difference in the γ-ray widths for these decays can be explained by simple nuclear structure considerations. Both beta decays are characterized by the $(\pi h_{11/2})^4 \rightarrow (\pi h_{11/2})^3(\nu h_{9/2})^1$ spin-flip transition. For $^{149}Er^{m}$ decay, the remaining odd neutron is in the $\nu h_{11/2}$ orbital and can deexcite by the unhindered $(\nu h_{9/2})^1(\nu h_{11/2})^{11} \rightarrow (\nu h_{11/2})^{12}$ $M1$ transition which competes favorably with proton decay. For $^{149}Er^{g}$ decay, the remaining odd neutron is in the $\nu s_{1/2}$ orbital and the recoupling of the two neutrons is severely retarded. In that case proton decay will be enhanced with respect to γ-ray deexcitation as is observed. The level density near 4–5 MeV, populated by $^{149}Er^{m+g}$ decay, in ^{149}Ho is low enough to create fine structure in the delayed proton spectrum. This is true for both decays; however, the arguments outlined above show why the structured delayed proton emission from $^{149}Er^{m}$ decay is strongly suppressed. The level density at higher excitations in ^{149}Ho is much larger, so fine structure is no longer expected for protons originating from that region. This was observed in both decays. Similar results were also measured in the decays of $^{147}Dy^{g+m}$ (Ref. 7) and $^{151}Yb^{g+m}$.[5] In those decays the structured protons were associated with the low-spin decay and the protons from the isomer decay were unstructured.

ACKNOWLEDGMENTS

We express our thanks to the staff of the SuperHILAC accelerator of the Lawrence Berkeley Laboratory, and L. F. Archambault and A. A. Wydler for their excellent and efficient cooperation. The work at Lawrence Berkeley Laboratory was supported by the Office of Energy Research, Division of Nuclear Physics of the Office of High Energy and Nuclear Physics of the U. S. Department of Energy under Contract No. DE-AC03-76SF00098. Oak Ridge National Laboratory is operated by Martin Marietta Energy Systems, Inc. for the U. S. Department of Energy under Contract No. DE-AC05-84OR21400.

*On leave from University of Helsinki, SF00180, Finland.
†On leave from Soreq Nuclear Research Center, Yavne 70600, Israel.

[1]R. B. Firestone, R. C. Pardo, R. A. Warner, Wm. C. McHarris, and W. H. Kelly, Phys. Rev. C **25**, 527 (1982).
[2]R. B. Firestone, R. A. Warner, Wm. C. McHarris, and W. H. Kelly, Phys. Rev. C **11**, 1864 (1975).
[3]K. S. Toth, D. M. Moltz, Y. A. Ellis-Akovali, C. R. Bingham, M. D. Cable, R. F. Parry, and J. M. Wouters, Phys. Rev. C **25**, 667 (1982).
[4]K. S. Toth, A. E. Rainis, C. R. Bingham, E. Newman, H. K. Carter, and W. D. Schmidt-Ott, Phys. Lett. **56B**, 29 (1975).
[5]K. S. Toth, Y. A. Ellis-Akovali, J. M. Nitschke, P. A. Wilmarth, P. K. Lemmertz, D. M. Moltz, and F. T. Avignone III, Phys. Lett. B **178**, 150 (1986).
[6]K. S. Toth, D. M. Moltz, E. C. Schloemer, M. D. Cable, F. T. Avignone, and Y. A. Ellis-Akovali, Phys. Rev. C **30**, 712 (1984).
[7]D. Schardt, P. O. Larsson, R. Kirchner, O. Klepper, V. T. Koslowsky, E. Roeckl, K. Rykaczewski, K. Zuber, N. Roy, P. Kleinheinz, and J. Blomqvist, in *Proceedings of the 7th International Conference on Atomic Masses and Fundamental Constants (AMCO7), Darmstadt-Seeheim, 1984,* edited by O. Klepper (Technische Hochshule Darmstadt, Darmstadt, 1984).
[8]K. S. Toth, Y. A. Ellis-Akovali, F. T. Avignone III, R. S. Moore, D. M. Moltz, J. M. Nitschke, P. A. Wilmarth, P. K. Lemmertz, D. C. Sousa, and A. L. Goodman, Phys. Rev. C **32**, 342 (1985).
[9]J. M. Nitschke, Nucl. Instrum. Methods **206**, 341 (1983).
[10]J. T. Routti and S. G. Prussin, Nucl. Instrum. Methods **72**, 125 (1969).
[11]R. A. Belshe and M. K. Lee, Nucl. Instrum. Phys. Res. **A253**, 65 (1986).
[12]R. A. Belshe, SUSIE Reference Manual, Lawrence Berkeley Laboratory, Report PUB-3061, 1987.
[13]R. A. Belshe, EVA Reference Manual, Lawrence Berkeley Laboratory, Report PUB-3062, 1987.
[14]W. Bambynek, B. Crasemann, R. W. Fink, H.-U. Freund, H. Mark, C. D. Swift, R. E. Price, and P. V. Rao, Rev. Mod. Phys. **44**, 716 (1972).
[15]N. B. Gove and M. J. Martin, At. Data Nucl. Data Tables A **10**, 205 (1971).
[16]G. Azuelos and J. E. Kitching, At. Data Nucl. Data Tables **17**, 103 (1976).
[17]J. B. Cumming, National Academy of Sciences Report NAS-NS **3107**, 1962, p. 25.
[18]A. H. Wapstra and G. Audi, Nucl. Phys. **A432**, 140 (1985).
[19]S. Liran and N. Zeldes, At. Data Nucl. Data Tables **17**, 431 (1976).
[20]G. D. Alkhazov, A. A. Bykov, V. D. Wittmann, V. E. Starodubsky, S. Yu. Orlov, V. N. Panteleyev, A. G. Polyakov, and

V. K. Tarasov, Nucl. Phys. **A438**, 482 (1985).
[21]P. Hornshoj, K. Wilsky, P. G. Hansen, B. Jonson, and O. B. Nielsen, Nucl. Phys. **A187**, 609 (1972).
[22]J. Wilson, S. R. Faber, P. J. Daly, I. Ahmad, J. Borgreen, P. Chowdhury, T. L. Khoo, R. D. Lawson, R. K. Smither, and J. Blomqvist, Z. Phys. A **296**, 185 (1980).
[23]J. A. Szucs, M. W. Johns, and B. Singh, Nucl. Data Sheets **46**, 1 (1985).
[24]G. D. Alkhazov, A. A. Bykov, V. D. Wittmann, S. Yu. Orlov, and V. K. Tarasov, Phys. Lett. **157B**, 350 (1985).
[25]J. M. Nitschke, P. A. Wilmarth, J. Gilat, K. S. Toth, and F. T. Avignone III, Phys. Rev. C **37**, 2694 (1988).
[26]J. Honkanen, J. Aysto, V. Koponen, P. Taskinen, K. Eskola, S. Messelt, and K. Ogawa, in *Nuclei Far from Stability (Rousseau Lake, 1987),* Proceedings of the Fifth International Conference on Nuclei Far from Stability, AIP Conf. Proc. No. 164, edited by I. S. Towner (AIP, New York, 1988), p. 640.
[27]H. Hama, M. Yoshii, K. Taguchi, T. Ishimatsu, T. Shinozuka, and F. Fujioka, in *Nuclei Far from Stability (Rousseau Lake, 1987),* Proceedings of the Fifth International Conference on Nuclei Far from Stability, AIP Conf. Proc. No. 164, edited by I. S. Towner (AIP, New York, 1988), p. 650.
[28]T. Sekina, J. Cerny, R. Kirchner, O. Klepper, V. T. Koslowsky, A. Plochocki, E. Roeckl, D. Schardt, B. Sherrill, and B. A. Brown, in *Nuclei Far from Stability (Rousseau Lake, 1987),* Proceedings of the Fifth International Conference on Nuclei Far from Stability, AIP Conf. Proc. No. 164, edited by I. S. Towner (AIP, New York, 1988), p. 654.